2013

Non-Cytotoxic Antibacterial Silver–Coumarin Complex Doped Sol–Gel Coatings

Swarna Jaiswal
Technological University Dublin, swarna.jaiswal@tudublin.ie

Kunal Bhattacharya
Technological University Dublin

Maeve Sullivan
Institute of Technology, Tallaght

Maureen Walsh
Institute of Technology, Tallaght

Bernadette Creaven
Institute of Technology, Tallaght

Non-cytotoxic antibacterial silver-coumarin complex doped sol-gel coatings

Swarna Jaiswal[a,b], Kunal Bhattacharya[c], Maeve Sullivan[d], Maureen Walsh[d], Bernie Creaven[d], Fathima Laffir[e,] Brendan Duffy[a]*, and Patrick McHale[b]

[a]Centre for Research in Engineering Surface Technology (CREST), FOCAS Institute, Dublin Institute of Technology, Dublin 8, Ireland

[b]School of Biological Sciences, Dublin Institute of Technology, Kevin Street, Dublin 8, Ireland

[c]Nanolab Research Centre, FOCAS Institute, Dublin Institute of Technology, Dublin 8, Ireland

[d]Centre for Pharmaceutical R&D, School of Science, Institute of Technology, Tallaght, Dublin 24, Ireland

[e]Materials & Surface Science Institute, University of Limerick, Dublin, Ireland

*Corresponding author: Dr. Brendan Duffy; Tel: +353-1-402-7964;

E-mail: brendan.duffy@dit.ie

Abstract

Microbial colonization on clinical and industrial surfaces is currently of global concern and silane based sol-gel coatings are being proposed as potential solutions. Sol-gels are chemically inert, stable and homogeneous and can be designed to act as a reservoir for releasing antimicrobial agents over extended time periods. In the present study, silver nitrate (AgN) and a series of silver coumarin complexes based on coumarin-3-carboxylatosilver (AgC) and it's 6,7 and 8 hydroxylated analogues (Ag6, Ag7, Ag8) were incorporated into sol-gel coatings. The comparative antibacterial activity of the coatings was determined against meticillin resistant *Staphylococcus aureus* (MRSA) and multidrug resistance *Enterobacter cloacae* WT6. The percentage growth inhibitions were found in the range of 9.2 (±2.7) % to 66.0 (±1.2) % at low silver loadings of 0.3% (w/w) with *E. cloacae* being the more susceptible. Results showed that among the Ag coumarin complexes, the Ag8 doped coating had the highest antibiofilm property. XPS confirmed the presence of silver in the nanoparticulate state (Ag^0) at the coating surface where it remained after 4 days of exposure to bacterial culture. Comparative cytotoxicity studies revealed that the Ag-complex coatings were less toxic than the AgN coating. Thus, it can be concluded that a sol-gel matrix with Ag-coumarin complexes may provide non-toxic surfaces with antibacterial properties.

Keywords: Antibacterial, Cytotoxicity, Ag-coumarin complexes, Surface coating

1. Introduction

A critical problem facing the biomaterials sector is how to retard bacterial growth and prevent biofilm formation on susceptible surfaces. Bacteria can adhere to surfaces, multiply and form a compact biofilm matrix, which protects the underlying bacteria from the action of antibiotics, antibacterial agents and host defence mechanisms. If this occurs with biomedical devices, such as prosthetic implants and catheters, it can result in serious infection, leading to implant failure [1, 2]. The risk of this occurring can be reduced by the biomedical devices having antimicrobial surfaces in the form of treatments or coatings which prevent microbe adhesion and proliferation [3]. For such applications, coatings need to combine antibacterial efficacy and low toxicity to eukaryotic cells. Various strategies such as (a) ionized/bound surface modification [6], (b) incorporated metals in the form of salts [7], complexes [8] and nanoparticles [9, 10] and (c) organic molecules [11] have been developed to deliver a coating that can inhibit or remove bacteria [4, 5],

The sol-gel process can be used to form nano structured inorganic films (typically 200nm to 10μm in overall thickness) that are more resistant than metals to oxidation, corrosion, erosion and wear while also possessing good thermal and electrical properties [12]. The technology has gained popularity very recently for the preparation of porous coatings at relatively low temperature with desirable surface chemistries, chemical durability [13] and thermal stability [14]. One of the most useful opportunities for sol-gels is the inclusion of antibacterial metals and carboxylated organic coumarin molecules which could produce an effective biomaterial coating.

A number of recent studies have highlighted naturally derived and synthetic coumarin (2H-1-benzopyran-2-one) derivatives with potential antimicrobial [15, 16] and antifungal activities

[17]. There are a number of commercially available coumarin-based antibiotics such as novobiocin, clorobiocin and coumermycin A_1. It has been reported that coordination of metal ions to therapeutic agents improves their efficacy and accelerates bioactivity. Coumarin derivatives can yield a wide variety of metal complexes with different coordination modes, spectroscopic properties and potential applications. In particular, coumarin-derived carboxylate ligands can coordinate to various d-block metal ions in a number of ways. Copper (II) complexes have binuclear bridged structures while silver (I) complexes are also binuclear however the carboxylate group has a unidentate binding mode. Silver (I) coumarin complexes possess excellent antimicrobial activity even though the ligands themselves are inactive [15, 18].

In this paper, silver nitrate and carboxylated coumarin complexes containing Ag were incorporated into sol-gel matrixces to produce homogeneous coatings in microtiter wells and on glass slides. These were analyzed for biological activity and compared with blank control equivalents. The chemical and biological properties of the coating surfaces were analyzed. The coatings were examined by scanning electron microscopy (SEM) after exposure to biofilm forming *Staphylococcus epidermidis* CSF 41498. Furthermore, the chemical composition of the coatings before and after 4 days bacterial exposure was determined by X-ray photoelectron spectroscopy (XPS). The release rate of silver ions (Ag^+) from the coatings was studied and correlated with the antibacterial efficacy data. Finally, the cytotoxicity of the various coatings for human keratinocyte cells was determined.

2. Experimental

2.1. Complex synthesis

The complexes were prepared as described previously [15, 18]. Their structure and purity were confirmed by thin-layer chromatography, infrared analysis, ^{1}H-and ^{13}C-NMR spectroscopy and elemental analysis.

2.2. Preparation of sol-gels

All chemicals were purchased from Aldrich (Ireland).

(a) *Stock (blank) sol-gel:* A blank, additive-free sol-gel, serving as a control, was prepared by mixing MTEOS with ethanol for 5 min followed by the gradual addition of nitric acid and water as described previously [19]. The mixture was stirred continuously for 24 h.

(b) *Ag- doped sol-gels*: Different levels of a dried silver salt and four silver-coumarin complexes were doped into aliquots of stock sol-gel to give doping concentrations of 0.7, 0.5 and 0.3% (w/w) of silver with respect to the final coatings weight (allowing for solvent loss and curing). The modified sol-gel solutions were stirred for 24 h in dark conditions to complete the formulation.

The silver salt gel (AgN) was made with silver nitrate and the sol-gel. The complex doped sols were denoted as AgC, Ag6, Ag7 and Ag8 representing [Ag(Cca)] coumarin-3-carboxylatosilver (I), [Ag(6OHCca)] 6-hydroxycoumarin-3-carboxylatosilver (I), [Ag(7OHCca)] 7-hydroxycoumarin-3-carboxylatosilver (I) and [Ag(8OHCca)] 8-hydroxycoumarin-3-carboxylatosilver(I) respectively. The complexes required the additional use of 5% Dimethyl sulfoxide (DMSO) in ethanol, as a solvent for solubility purposes.

2.3. Coating procedure

The sol-gels were applied as coatings on microtitre wells and 1 x 1 cm glass slides. Sol-gels (200 µl) were dispensed into a microtiter plate (Nunc, Denmark) and cured in a vacuum tight oven at the 70°C for 3 days [19]. The sol-gel were spin coated onto the glass slides (Specially coating instrument systems-spin coat G3P-8) at 1000 rpm with 5 sec RAM and 1 min dwell time and cured at 70°C for 3 days. All coatings were stored at 4°C prior to biofilm studies and XPS analysis.

2.4. Antibacterial activity assay

The test bacteria chosen multidrug resistant (ampicillin, gentamicin and ceftazidine) *Enterobacter cloacae* WT6, meticillin resistant *S. aureus* (MRSA) ATCC 43300 and *S.. epidermidis* CSF 41498) were clinically significant antibiotic resistant strains. They were grown, sub-cultured and maintained on Mueller-Hinton agar (LAB M) and stored at 4°C. For the experiment, a single colony of each organism was inoculated into Mueller-Hinton broth (MHB, 10 ml) and incubated overnight (24 h) at 37°C with shaking at 200 rpm. The OD_{600} of the culture was adjusted to 0.132 (corresponding to 1.5×10^8 CFU.ml^{-1}) using sterile MHB and further diluted to give a final working concentration of 1.5×10^6 CFU.ml^{-1}.

The antibacterial activity of the Ag-doped sol-gel coatings against the test bacteria was determined using the microtiter plate method. Test bacteria (100 µl) from the 10^6 CFU ml^{-1} suspensions were added to all test wells. A blank well containing the respective cured Ag-doped sol-gel coating with sterile MHB (100 µl) and a negative control well containing the blank sol-gel with the bacterial suspension (100 µl) were used. The microtiter plates were incubated for 24 h at 37ºC.

The antibacterial activities of the different coatings were determined by calculating the percentage inhibition of growth [20]. The coating with the lowest incorporated metal concentration that completely inhibited bacterial growth after 24 h was considered the minimum incorporated inhibitory concentration (MIIC). The minimum incorporated bactericidal concentration (MIBC) was determined by the modified imprint method where the well contents (10 µl) were sub cultured onto MHA plates. The MIBC was considered to be the lowest concentration that produced no visible bacterial growth on the MHA plate after 24 h at 37°C indicating 99.5% killing of the original inoculum. All experiments were performed in triplicate and repeated at least twice.

2.5. Mathematical modelling of bacterial growth

2.5.1. Relation between turbidity and viable count

In order to convert the OD to log CFU.ml^{-1}, a relationship between OD_{600} nm and viable count for the test bacteria was determined [21]. An aliquot (200 µl) of bacterial suspension (1.5×10^6 CFU ml^{-1}) was dispensed into the wells of the 96-well coated microtiter plate. Every hour, the OD of the well contents was read and an aliquot (100 µl) from each of 3 wells was transferred into maximum recovery diluent (MRD, 900 µl). This was further tenfold diluted, and dilutions (100 µl) were plated out on MHA plates and incubated at 37ºC for 24 h, in order to determine the number of CFUml^{-1}. A standard curve (OD_{600} nm vs. log CFU.ml^{-1}) was drawn from the results obtained.

2.5.2. Growth curve kinetics

The turbidity OD was measured at 600nm at time intervals of 30 min, with 20 sec agitation before each measurement, on a Powerwave microplate spectrophotometer (Powerwave, Biotek)

driven by Gen5 reader control and data analysis software. The OD values were converted to log CFU ml^{-1} by the standard curve as described above in 2.5.1.

Predictive modelling can be used to describe the growth curves of the microorganisms over finite time periods. The growth characteristics can be determined using established iterative techniques using a least squares method. In general bacterial growth often shows a phase where specific growth rate starts at a value of zero for a time period called a lag time (λ). Thereafter growth accelerates exponentially at a maximum rate (μ_{max}) before slowing and stopping (stationary period) so that a maximum colony count or asymptote (A) is reached. The value A therefore represents the maximum colony count achievable under the experimental conditions. The characteristic shape of such curves become sigmoidal when colony counts are expressed in logarithmic terms. There are several models, which have been used to describe the sigmoid growth curve of a microorganism such as the Baranyi, Gompertz or Logistic models [22]. In general the Gompertz model is regarded as the most suitable to describe such microbial growth curves due to its simplicity and the low correlation, or interdependence, of the characteristic parameters.

For the purposes of this work the modified Gompertz equation [22] was fitted to the logarithm of the cell concentration in order to estimate the maximum specific growth rates (μ_{max}) and lag phase (λ) of *E. cloacae* WT6 and MRSA ATCC 43300 using STATGRAPHICS Centurion XV (StatPoint Technologies, Inc., Warrenton, VA) statistical software. The model is described by the equation (*Eq.* 1):

$$\log\left(\frac{N}{N_0}\right) = A \times \exp\left\{-\exp\left[\frac{\mu \times e}{A}(\lambda - t) + 1\right]\right\} \qquad (1)$$

where μ is the maximum specific growth rate of cell population, A is the log increase of the population and λ is the delayed time variable (lag phase), N is the CFU ml^{-1} at any time t, N_0 is the initial CFU ml^{-1}.

2.6. Biofilm inhibition assay

S. epidermidis CSF 41498 (500µl of 1.5×10^6 CFU ml^{-1}) was pipetted into the coated microtiter wells (24 well plate) and incubated at 37°C for 4 days. The control wells consisted of MTEOS coating with either sterile or bacterial loaded MHB. After incubation, the suspensions were removed and the wells gently rinsed thrice with sterile water to remove loosely associated bacteria. The biofilms retained on the coating surfaces were stained with 1% (w/v) crystal violet solution (500 µl) for 45 min. After staining, coatings were washed thrice with sterile distilled water. At this point, biofilms were visible as purple rings formed on the surface of each well. Biofilm production was analysed by adding 95% ethanol (500 µl) for 10 min to destain the wells. Aliquots (100 µl) of these were transferred to wells of another microtiter plate and OD measured at 570nm. The absorbance values were considered to be directly proportional to the amount of biofilm biomass retained on the coating surface. The results obtained were compared to those for an antimicrobial-free control coating to determine the relative reduction in biofilm growth.

2.7. Microscopic biofilm assay

Coated glass slides (1 cm^2) spin coated with Ag8 sol-gel, of concentrations 0.5 and 0.7% (w/w), and the blank sol-gel were placed in sterile petri dishes and *S. epidermidis* CSF 41498 (5 ml, 1.5×10^6 CFU ml^{-1}) was added. After incubation at 37°C for 4 days, the slides were removed, rinsed gently with sterile water, mounted on a stub and gold coated (Cressington 208HR sputter coater) for analysis of the bacterial morphology using a Hitachi SU6600 scanning electron microscope (SEM) operating at 15 KeV.

2.8. Quantitative elementary analysis

The surface chemistry of the coatings was analysed by XPS using a Kratos AXIS 165 spectrometer with monochromatic Al Kα radiation of energy 1486.6 eV. High resolution spectra were taken at fixed pass energy of 20 eV. Binding energies were determined using C 1s peak at 284.8 eV as charge reference. For construction and fitting of synthetic peaks of high resolution spectra, a mixed Gaussian-Lorenzian function with a Shirley type background subtraction were used.

2.9. Evaluation of silver ion release rate

The release rate of the silver ions from the sol-gel coatings into sterile de-ionised water was analysed by ICP-AES (Varian Liberty 150). Plastic wells were attached to the surface of Ag8 and AgN sol-gel coated glass slides (0.7 % (w/w)) using an epoxy fixative (Araldite, Huntsman (UK)) and left for 24 hours [23]. Water (5ml) was added to the wells (with a surface area of 4.9 cm^2) and the slides were incubated at 37°C. Samples were removed and replaced with fresh water aliquots after 1, 4, 8, 12, 24, 48, 72 and 96 hours. All leachates were stored at 4°C prior to pooling and acidification with nitric acid (0.1M) for analysis as a single batch by ICP-AES, using a certified stock silver standard solution (ARISTAR® silver, BDH, England) for calibration purposes.

2.10 *In vitro* cell culture

Immortalized non-cancerous human keratinocyte (HaCat) cells were cultured in Dulbecco's Modified Eagle's Medium Nutrient Mixture F-12 HAM(DMEM-F12) supplemented with 10% foetal bovine serum (FBS) and antibiotic supplement (45 IU ml^{-1} penicillin and 45 IU ml^{-1} streptomycin) at 37°C in 5% CO_2.

2.10.1. Cytotoxicity assay

The coated microtiter wells (24 wells) were sterilized by UV radiation for 2 h. HaCat cells (500 µl of 1×10^5 cells ml^{-1} and 8×10^4 cells ml^{-1}) were added to the wells and incubated at 37°C for (24 and 48h) in 5% CO_2. MTEOS coated wells with HaCat cells were used as negative controls whereas cells with cis-diamminedichloroplatinum(II) (13µM) served as a positive control. Following the completion of the exposure time, an Alamar Blue (AB) assay was performed according to literature [24]. Briefly, wells were rinsed with phosphate buffered saline (PBS) and 500µl of AB medium (5% v/v in fresh culture medium without fetal bovine serum (FBS) or supplements) were added. After 3 h of incubation, the AB fluorescence was measured at the excitation and emission wavelengths of 540 and 595 nm respectively, in a microplate reader (TECAN GENios, Grodig, Austria). Six replicate wells were used for each control and test, per microtiter plate, and the experiment was repeated at least twice. The percentage cell viability was determined for all test coatings.

2.11 Statistical analysis

All the statistical analyses were done using STATGRAPHICS Centurion XV. The statistical significance (95% confidence level ($p < 0.05$)) between the means for the different Ag-coumarin complexes was determined by ANOVA followed by multiple range tests (least significant difference). Where inter-sample variation was not significant a group (denoted as a, b or c *etc*.) was defined. Within each concentration, all samples denoted as "a" would be equivalent but statistically different from samples denoted "b" and so on

3. Results and discussion

The sol-gels (both blank and Ag doped) formed clear uniform coatings in the microtitre wells after curing at the optimised temperature. Following curing the AgN coatings remained clear

while the Ag-coumarin doped coatings developed a slight yellow colouring, characteristic of silver nanoparticles (Ag^0). It may be hypothesized that the Ag-coumarin complexes form weak bonds with the MTEOS at the low pH of 3-4, and may dissociate into silver ion (Ag^+) and coumarin (Cca). The curing temperature promoted the development of the yellowing indicating that there is a thermodynamic process occurring.

3.1. Antibacterial activity

The percentage growth inhibition of *E. cloacae* WT6 and MRSA by the test sol-gel coatings containing varying doping levels (0.3%, 0.5% and 0.7% (w/w)) was determined. There was a complete absence of bacterial growth for all Ag based coatings at a loading level of 0.7% (w/w). At 0.5% (w/w) loadings significant levels of inhibition (>89%) were observed in all Ag coatings (Table 1), whereas at 0.3% (w/w) partial inhibition of bacterial growth was observed (critical concentration). The MIICs and MIBCs of all Ag doped coatings were found to be 0.5% (w/w) against both test bacteria. Results showed that Cca had no significant antibacterial activity. Among the Ag-coumarin complexes, Ag8 coatings showed significantly ($p < 0.05$) higher percentage growth inhibition at the critical concentration (0.3% (w/w) although somewhat lower than the base reference AgN.

3.2. Growth curve kinetics

Traditional microbial enumeration techniques are time consuming and therefore, mathematical models are regularly used to establish the kinetic parameters of survival curves of microorganisms. The empirical sigmoid type models such as the modified Gompertz, Logistic or Baranyi models have been used to fit bacterial growth [25], however, these models are usually only applied to food processing and food safety studies. As per the author knowledge this is first

time modeling has been used for the analysis of delaying or inhibition of bacterial growth on the coating surfaces.

Different concentrations of incorporated Ag-coumarin complexes showed variable levels of bacterial inhibition over 24 h of incubation (Fig.1). The coatings showed a strong antagonizing effect on the test bacteria studied, displaying a significant dose-dependent relationship with an increase in the lag phase duration (λ) and corresponding decrease in the exponential growth rate (μ). A modified Gompertz model was applied to estimate the delay or inhibition in bacterial (MRSA and *E. cloacae*) growth. In most cases, the correlation (R^2) values for the models were greater than 99% indicating a good fit to the experimental data (Table 2). It was also established that the maximum specific growth rate (μ_{max}), was significantly ($p < 0.05$) reduced in the presence of the Ag doped coatings. Reduction in the μ_{max} for the Ag-coumarin coatings ranged from 41to 56% for *E. cloacae* and 18 to 41% for MRSA with respect to control. The corresponding reductions for AgN were higher at 62% and 95% respectively

At the critical concentration (0.3%) the Ag-coumarin coatings increased the lag phase from 1 to 3.81 h for *E. cloacae* and from 2.09 to 5.35 h for MRSA. Among the Ag-coumarin coatings Ag8 was the most efficient, increasing the lag phase of *E. cloacae* and MRSA by 64.68 % and 191.75% with respect to control. It is hypothesized that small structural differences in the Ag-complexes caused some changes in the biological activity. The position of the hydroxyl group in these Ag-complexes is known to contribute significantly to antimicrobial activity [17].

3.3 Biofilm inhibition assay

Biofilm formation is a multi-factorial process involving the adhesion of bacterial cells to a host substrate, followed by subsequent attachment and colonisation [23]. *S. epidermidis* is the most

common bacterium isolated from medical devices such as vascular catheters, prosthetic implants and intrauterine devices [26]. Surface colonisation can be inhibited either by direct surface coatings or with entrapped agents that are gradually released. Such hygienic coatings can be employed on environmental surfaces and medical devices. The percentage inhibition of *S. epidermidis* biofilm growth on Ag doped sol-gel coatings is displayed in Fig. 2. In comparison to the blank control, a reduction in biofilm formation of about 25-80% was observed in the presence of Ag-coumarin coatings across the studied concentration range (0.3% to 0.7% (w/w)).

Among the Ag-doped coatings, maximum biofilm inhibition was observed with Ag8 while AgC showed the least inhibition. In terms of performance, there was a clear ranking among the Ag-coumarin sol-gel coatings at the all concentrations, namely Ag8> Ag7 > Ag6 > AgC, with the last two position reversed at 0.3% (w/w). Interestingly the improvement in inhibition of the Ag-coumarin coatings with concentration was not as clear as with the AgN coatings. AgN coatings showed antibiofilm activity from 21% at 0.3% (w/w) up to 73% at 0.7%. It was also evident from the results that there was significant ($p > 0.05$) difference between Ag8, Ag7 and AgN coatings at 0.3% and 0.5% whereas; at 0.7% AgN there was not.

3.4. Microscopic biofilm assay

The effect of silver ion release from the Ag8 coatings was studied by SEM (Fig. 3). After 4 days of incubation, the biofilm was fully established on the blank control coating and the glass slide was covered with adherent *S. epidermidis* CSF 41498 (Fig. 3a). Silver ion release from the doped Ag8 reduced the bacterial colonisation on the coating surface and distinctive crystalline precipitates were seen (Fig. 3b & 3c). These may be due to insoluble adherent salt crystals on the

coating surface. Extraneous matter such as chloride from the culture medium may have coupled with some of the released silver ions to form silver chloride at the surface in the broth.

The Ag8 coating greatly reduced biofilm formation at 0.5% (Fig.3b) and produced a higher number of damaged bacterial cells at 0.7% (Fig.3c). These results were in agreement with some previous work, which showed that silver ions act at the peripheral area of *S. epidermidis* biofilm causing disruptive changes that destabilize it [27]. Moreover, rapid elution was found to be critical as silver ions become inactive after binding with protein anions and polysaccharides in the biofilm.

3.5. Quantitative elementary analysis

To describe the antibacterial activity of a coating, an understanding of the surface properties and change in its chemical state are important. XPS was used to study the change in the surface chemical state of the most active coating (Ag8) and the reference (AgN) before and after immersion for 4 days in an *S. epidermidis* CSF 41498 culture. From the summary of the elemental composition given in Table 3 a significant increase in the relative carbon concentrations was seen after immersion in both cases. Before exposure carbon is present predominantly as hydrocarbon at a binding energy of 284.8 eV. However, after exposure the increase in carbon content is attributed to additional presence of carbonaceous species, C-O/C-N at ~ 286.5 eV and O=C=O/N-C=O at ~288.5 eV. Nitrogen related to these functional groups appears in the coatings at a binding energy of 400 eV after exposure in significant amounts (7.8 and 6.0 atomic %). These are likely to originate from proteinaceous species in the broth, assuming the damaged bacterial cell wall released protein into the broth. In addition, after exposure to the broth both coatings showed the presence of a small amount of sodium. However, the relative concentration of Na in Ag8 is notably less (0.4 %) than in AgN (1.6 %) perhaps indicating interaction of the coumarin ion with Na^+.

High resolution Ag 3d spectra of the Ag8 coating before and after exposure to *S. epidermidis* CSF 41498 are shown in Fig. 4a. The Ag 3d peak appears as a doublet of Ag 3d5/2 and Ag 3d3/2 at 368.1 eV and 374.5 eV respectively with a doublet separation of 6.0 eV characteristic of metallic Ag. After exposure, the Ag 3d5/2 peak shifts to a lower binding energy of 367.9 eV corresponding to oxidised Ag^{+} indicating that the Ag° has been released in the form of Ag^{+}. A similar trend in the binding energies was observed for the AgN doped coating (Fig.4b).

The relative composition of silver present in the Ag8 and AgN coatings was 0.1 % and 0.8 % pre bacterial incubation (Table 3). The silver content decreased significantly post incubation in the AgN coating, whereas in the Ag8 coating it showed the small change. This may suggest a continuous slow release of silver ion from Ag8 coating over the extended time period compared to AgN, which has a high initial silver release rate [28].

3.6. Evaluation of silver ion release rate

In order to possess effectiveness against microorganisms, silver ions should be capable of migrating from the hybrid matrix of the coatings. Fig.5 shows the release of silver from Ag8 and AgN coatings containing 0.7% (w/w) in to de-ionised water as a function of time at 37°C. The release of silver from both the Ag8 and AgN coatings was characterised by an initial high release followed by a sharp drop over the first 24 hours. The release rate from AgN decreased to less than 10ppb after 12 hours, whereas Ag8 maintained a release of >20ppb for 72 h, dropping to 13.9 ppb after 96 h. The results imply that the solubility of silver in the AgN coating is higher

than in the coumarin complex. From a design perspective a silver coating with a high release rate is not suitable as an antibacterial coating for biomaterials because the antibacterial agent can be quickly washed out [29].

After 96h, the controlled release rate of Ag^+ from Ag8 is still maintained at bactericidal levels. The release rate of Ag^+ depends on the concentration of nanoparticles and their diffusion to the coating surface. Rapid diffusion of the broth solution into the coating and higher accumulation of silver at the surface could result in a high metal release rate in the initial stages. Significant reduction in the release rate of Ag^+ in later stages can be explained by the rapid decrease of surface Ag particles and slower diffusion of the solution in the pores of the coating, thereby changing the Ag^+ release mechanism [30]. This diffusion release profile is consistent with porous systems and is in contrast to swelling materials which have a rapid ion release rate after a minimum release in the initial stage [31, 32].

The release of Ag^+ from silver nanoparticles is primarily a heterogeneous oxidation reaction involving oxygen chemisorption accompanied by electron transfer [33]. Therefore, methods that enhance or disrupt oxidation pathways are a promising route to controlled release. Several routes have been explored using macromolecules such as dextrans [20, 34], starch [35], and polymers [36, 37] which can block oxygen access. In this work, the Ag-coumarin coating serves as a source for Ag^+ in solution and the bound Ag^+ undergoes reversible adsorption-desorption influenced by the Ag^+ concentration. Coumarin coatings can both delay and extend ion release by accumulating and releasing Ag.

3.7. Cytotoxicity study

Cytotoxicity is a critical biocompatibility issue for synthesized compounds, including metal doped sol-gels. Published reports confirm that while Ag^{+} concentrations less than <35 ppb are bactericidal [38] higher concentrations between 1ppm and 10ppm may cause damage to human cells. This damage can range from low localised toxicity to conditions like argyria in higher doses (>4–6 g in the body) [39], Thus it is important to evaluate the cytotoxicity of the synthesized metal doped sol-gels coatings.

The study showed a dose-dependent response for all Ag coatings (Fig.6a and b), whereby the toxicity increased with increasing concentration from 0.3% to 0.7% (w/w). Following 24 h exposure to the Ag-coumarin coatings, the percentage cell viability was in the order of Ag7 ≥ Ag8 > Ag6 > AgC > AgN at almost all tested concentrations (0.3%, 0.5% and 0.7%) (Fig.6a). In the presence of Ag7 and Ag8 coatings, cell viability was up to 70-80 % at higher concentration (0.7%) with respect to negative control. After 48h of incubation (Fig.6b.) the cell viability for all coatings fell by approx 10-20% between 24 and 48 h. Importantly, the comparative cell viability was significantly ($P < 0.05$) higher for the Ag-coumarin coatings than for the AgN coating at all concentrations.

4. Conclusion

In summary, Ag doped sol-gels deliver a porous coating after curing at 70°C for 3 days. Antibacterial Ag-coumarins displayed activity within coatings even at a low concentration of 0.3% (w/w) with a reproducible difference in activity between tested complexes. Of the four coumarin coatings tested against the biofilm forming bacterium Ag8 sol-gel was shown to have significant antibiofilm properties at concentrations of 0.5 % and 0.7% (w/w). The Ag-coumarin

coatings showed less toxicity than AgN equivalents. Among all coatings Ag7 had the lowest toxicity while Ag8 had the highest antibacterial activity. XPS results confirmed that the silver was in its metallic form (Ag^0) within the Ag coumarin coating. There was a gradual release of Ag^+ from the Ag coumarin coating over an extended time period which maintained a higher efficacy. The coumarin reduced the toxicity of Ag in the coating; it is hypothesized that the prolonged release of Ag^+ is facilitated by the carboxylated coumarins, creating a less cytotoxic surface. These results provide evidence for the potential use of Ag-coumarin sol-gels coatings as biomedical coatings.

Acknowledgements

The authors would like to gratefully acknowledge Mr. Amit Kumar Jaiswal for assistance in mathematical modelling and Ms. Anne Shanahan for SEM imaging. The authors would also like to acknowledge the Dublin Institute of Technology, Dublin, Ireland for funding under the ABBEST scholarship program.

References

[1] V. Sambhy, M.M. MacBride, B.R. Peterson, A. Sen, Journal of the American Chemical Society. 128 (2006) 9798.

[2] D. Zhang, O. Lepparanta, E. Munukka, H. Ylanen, M.K. Viljanen, E. Eerola, M. Hupa, L. Hupa, Journal of Biomedical Materials Research. Part A 93 (2010) 475.

[3] C.H. Ho, J. Tobis, C. Sprich, R. Thomann, J.C. Tiller, Advanced Materials 16 (2004) 957.

[4] L. Zhao, P.K. Chu, Y. Zhang, Z. Wu, Journal of Biomedical Materials Research Part B: Applied Biomaterials 91 (2009) 470.

[5] L. Zhang, D. Pornpattananangkul, C.M.J. Hu, C.M. Huang, Current Medicinal Chemistry 17 (2010) 585.

[6] M. Chen, L.Y. Wang, J.T. Han, J.Y. Zhang, Z.Y. Li, D.J. Qian, The Journal of Physical Chemistry B 110 (2006) 11224.

[7] O. Choi, K.K. Deng, N. Kim, L. Ross, R.Y. Surampalli, Z. Hu, Water Res. 42 (2008) 3066.

[8] Y. Li, W.K. Leung, K.L. Yeung, P.S. Lau, J.K.C. Kwan, Langmuir 25 (2009) 13472.

[9] D. Ionita, M. Grecu, C. Ungureanu, I. Demetrescu, Applied Surface Science 257 (2011) 9164-9168.

[10] A. Travan, C. Pelillo, I. Donati, E. Marsich, M. Benincasa, T. Scarpa, S. Semeraro, G. Turco, R. Gennaro, S. Paoletti, Biomacromolecules 10 (2009) 1429.

[11] M. Vallet-Regí, M. Colilla, B. González, Chem. Soc. Rev. 40 (2011) 596.

[12] P.C.R.Varma, J. Colreavy, J. Cassidy, M. Oubaha, B. Duffy, C. McDonagh. Progress in Organic Coatings 66 (2009) 406.

[13] P.C. R. Varma, J. Colreavy, J. Cassidy, M. Oubaha, C. McDonagh, B. Duffy.Thin Solid Films 518 (2010) 5753.

[14] P.C. R. Varma, P. Periyat, M. Oubaha, C. McDonagh, B. Duffy. Surface & Coatings Technology 205 (2011) 3992.

[15] B.S. Creaven, D.A. Egan, K. Kavanagh, M. McCann, A. Noble, B. Thati, M. Walsh, Inorganica Chimica Acta 359 (2006) 3976.

[16] C. Gnerre, M. Catto, F. Leonetti, P. Weber, P.A. Carrupt, C. Altomare, A. Carotti, B. Testa, Journal of Medicinal Chemistry 43 (2000) 4747.

[17] B. Thati, A. Noble, R. Rowan, B.S. Creaven, M. Walsh, M. McCann, D. Egan, K. Kavanagh, Toxicology In Vitro 21 (2007) 801.

[18] B.S. Creaven, D.A. Egan, K. Kavanagh, M. McCann, M. Mahon, A. Noble, B. Thati, M. Walsh, Polyhedron 24 (2005) 949.

[19] S. Jaiswal, P. McHale, B. Duffy, Colloids and Surfaces B: Biointerfaces (2012).

[20] S. Jaiswal, B. Duffy, A.K. Jaiswal, N. Stobie, P. McHale, International Journal of Antimicrobial Agents 36 (2010) 280.

[21] A.K. Jaiswal, S. Gupta, N. Abu-Ghannam, S. Cox, Food Science and Technology International 17 (2011) 495.

[22] M.H. Zwietering, I. Jongenburger, F.M. Rombouts, K.Van 't Riet, Applied Environmental Microbiology 56 (1990)1875.

[23] N. Stobie, B. Duffy, J. Colreavy, P. McHale, S.J. Hinder, D.E. McCormack, Journal of Colloid and Interface Science 345 (2010) 286.

[24] S.P. Mukherjee, F.M. Lyng, A. Garcia, M. Davoren, H.J. Byrne, Toxicology and Applied Pharmacology 248 (2010) 259.

[25] S.Gupta, S. Cox, G. Rajauria, A.K. Jaiswal, N. Abu-Ghannam, Food and Bioprocess Technology (2011).

[26] P.S. Brunetto, K.M. Fromm, CHIMIA International Journal for Chemistry 62 (2008) 249.

[27] K. Chaw, M. Manimaran, F.E.H. Tay, Antimicrobial Agents and Chemotherapy 49 (2005) 4853.

[28] N Stobie, B Duffy, DE McCormack, J Colreavy, M Hidalgo, P McHale, SJ Hinder, Biomaterials 29 (2008) 963.

[29] B. Mahltig, D. Fiedler, P. Simon, Journal of the Textile Institute 102 (2011) 739.

[30] R. Kumar, H. Münstedt, Biomaterials 26 (2005) 2081.

[31] A. Babapour, B. Yang, S. Bahang, W. Cao, Nanotechnology 22 (2011) 155602.

[32] C. Damm, H. Münstedt, A. Rösch, Materials Chemistry and Physics 108 (2008) 61.

[33] J. Liu, D.A. Sonshine, S. Shervani, R.H. Hurt, ACS Nano (2010).

[34] Y.Q. Ma, J.Z. Yi, L.M. Zhang, Journal of Macromolecular Science, Part A: Pure and Applied Chemistry 46 (2009) 643.

[35] P. AshaRani, G. Low Kah Mun, M.P. Hande, S. Valiyaveettil, ACS Nano 3 (2008) 279.

[36] X. Cai, M. Lin, S. Tan, W. Mai, Y. Zhang, Z. Liang, Z. Lin, X. Zhang, Carbon (2012) (Doi: 10.1016/j.carbon.2012.02.002).

[37] R.B. Grubbs, Polymer Reviews 47 (2007) 197.

[38] A. Ewald, S.K. Glückermann, R. Thull, U. Gbureck, Biomedical Engineering Online 5 (2006) 22.

[39] G. Gosheger, J. Hardes, H. Ahrens, A. Streitburger, H. Buerger, M. Erren, A. Gunsel, F.H. Kemper, W. Winkelmann, C. von Eiff, Biomaterials 25 (2004) 5547.

Fig. 1. Fitting of the model to the inactivation of the bacteria by the coatings containing various Ag-complexes (control, AgC, Ag6, Ag7, Ag8 and AgN) at a concentration of 0.3 % (w/w) over 24 hours (a) *E. cloacae* WT 6 (b) MRSA.

Fig. 2. Percentage inhibition of biofilm forming *S.epidermidis* CSF41498 on sol-gel coatings Ag6, Ag7, Ag8, AgC and AgN at concentrations 0.3%, 0.5% and 0.7 % (w/w), after 4 days incubation

*Letter ($^{a-e}$) in each concentration are significantly different ($P < 0.05$) for various Ag-coumain complexes and AgN.

Fig. 3. SEM images of *S.epidermidis* CSF 41498 on (a) blank control coated glass slide, (b) Ag8 0.5% (w/w) coated slide and (c) Ag8 0.7% (w/w) coated slides.

Fig. 4. High resolution Ag 3d XPS spectra of (a) AgN doped coating (b) Ag8 doped coating before (dark curve) and after (grey curve) 4 days of exposure to biofilm forming *S.epidermidis* CSF 41498.

Fig. 5. Non-cumulative release rates of Ag into fresh DI H_2O from Ag8 and AgN coated glass slides as a function of time (determined by ICP emission spectroscopy).

Fig. 6. Cytotoxic response of HaCat cells after (a) 24 and, (b) 48 h of exposure to Ag-doped sol-gel coatings (Ag6, Ag7, Ag8, AgC and AgN) with increasing concentration of 0.3%, 0.5% and 0.7% (w/w).

*Letter ($^{a-e}$) in each concentration are significantly different ($P < 0.05$) for various Ag-coumain complexes and AgN.

Fig.1.

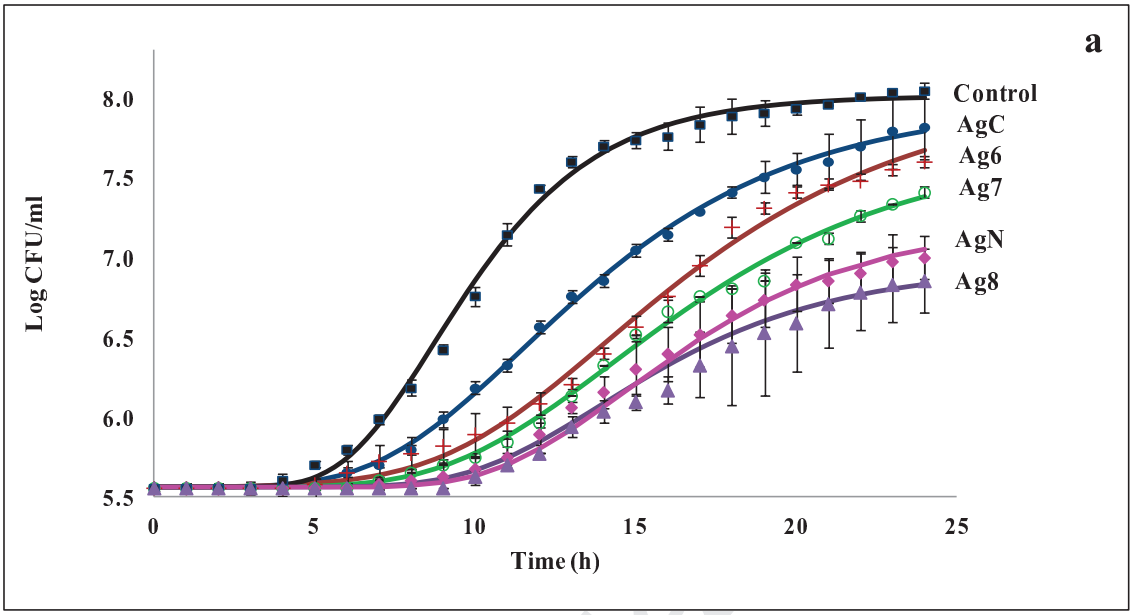

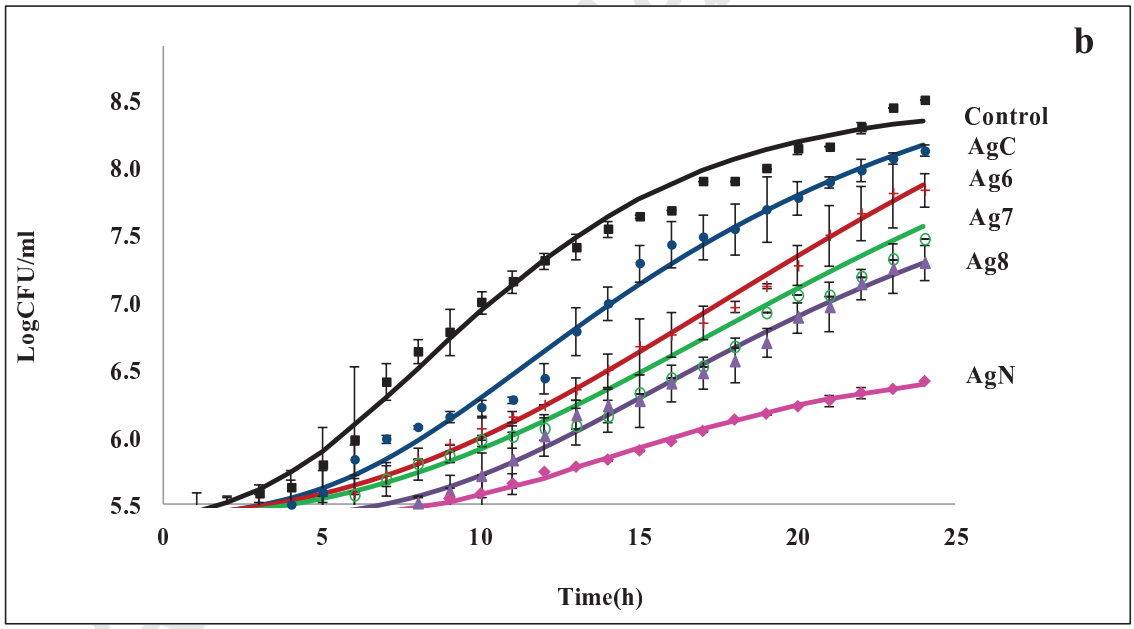

Fig. 2.

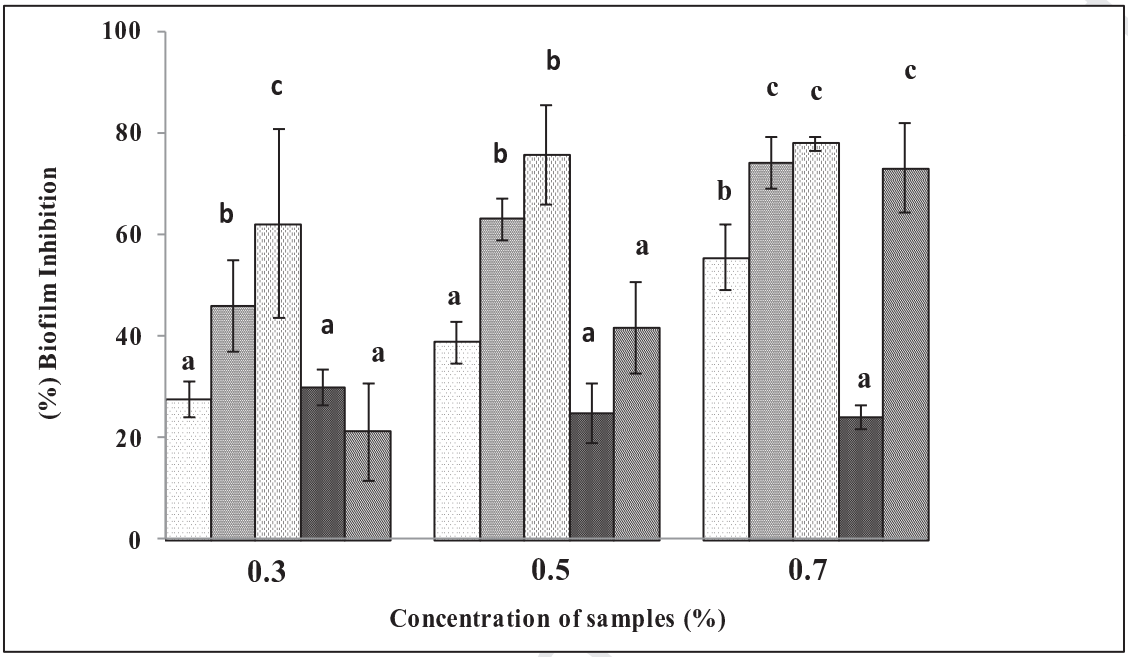

Fig. 3.

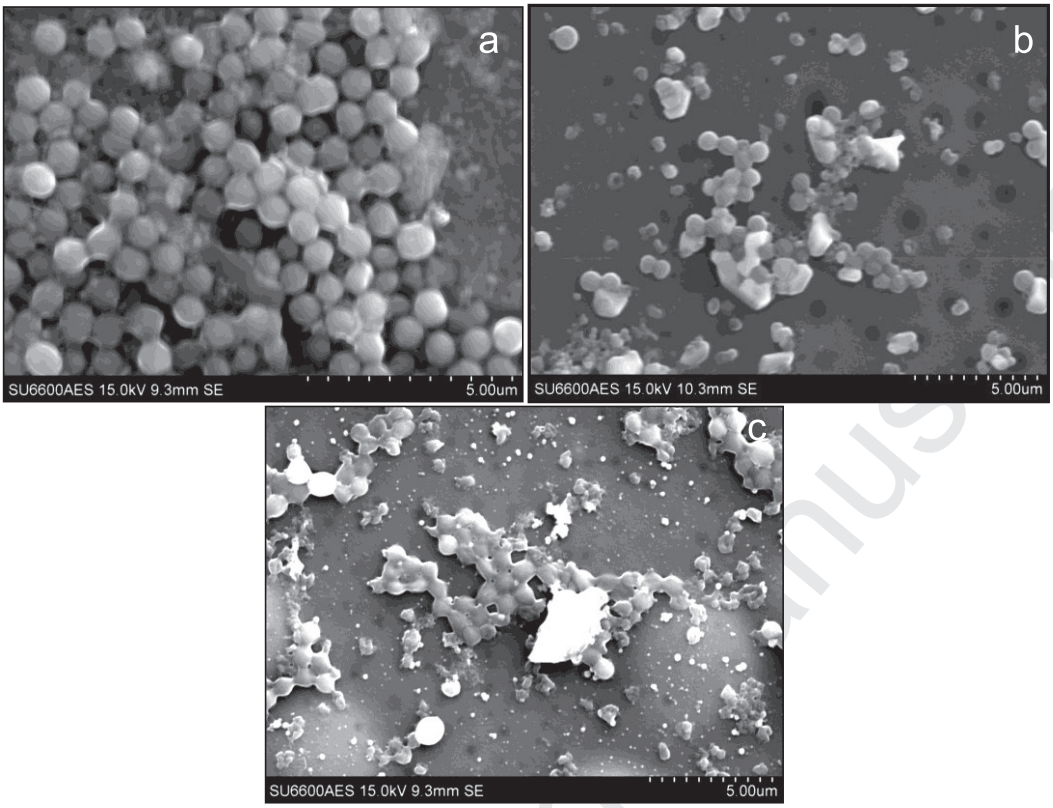

Fig. 4.

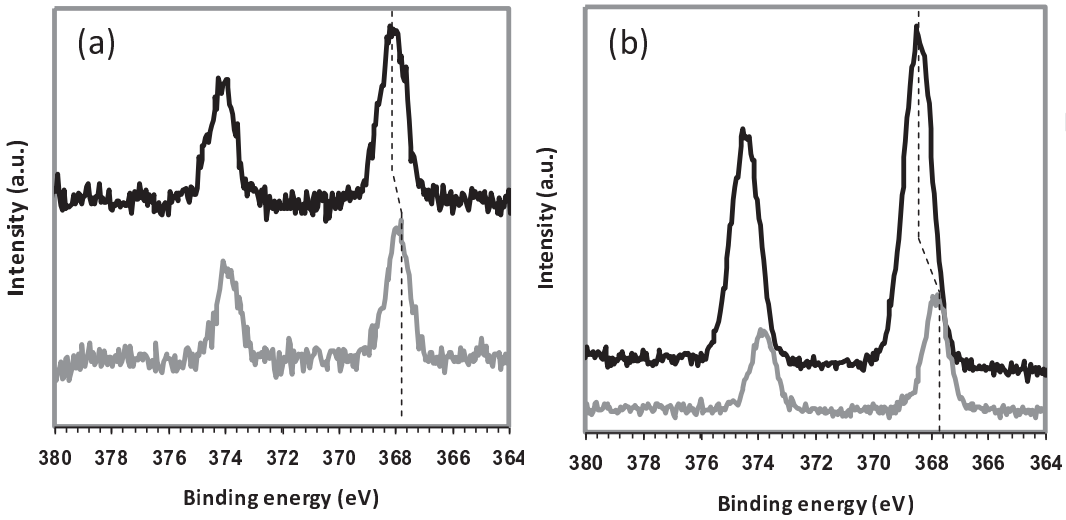

Fig. 5.

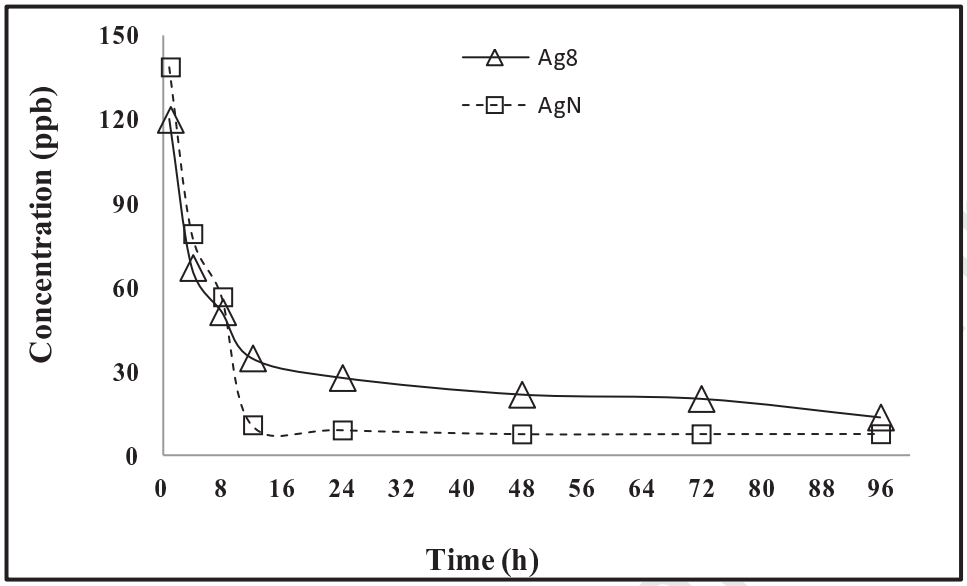

Fig. 6.

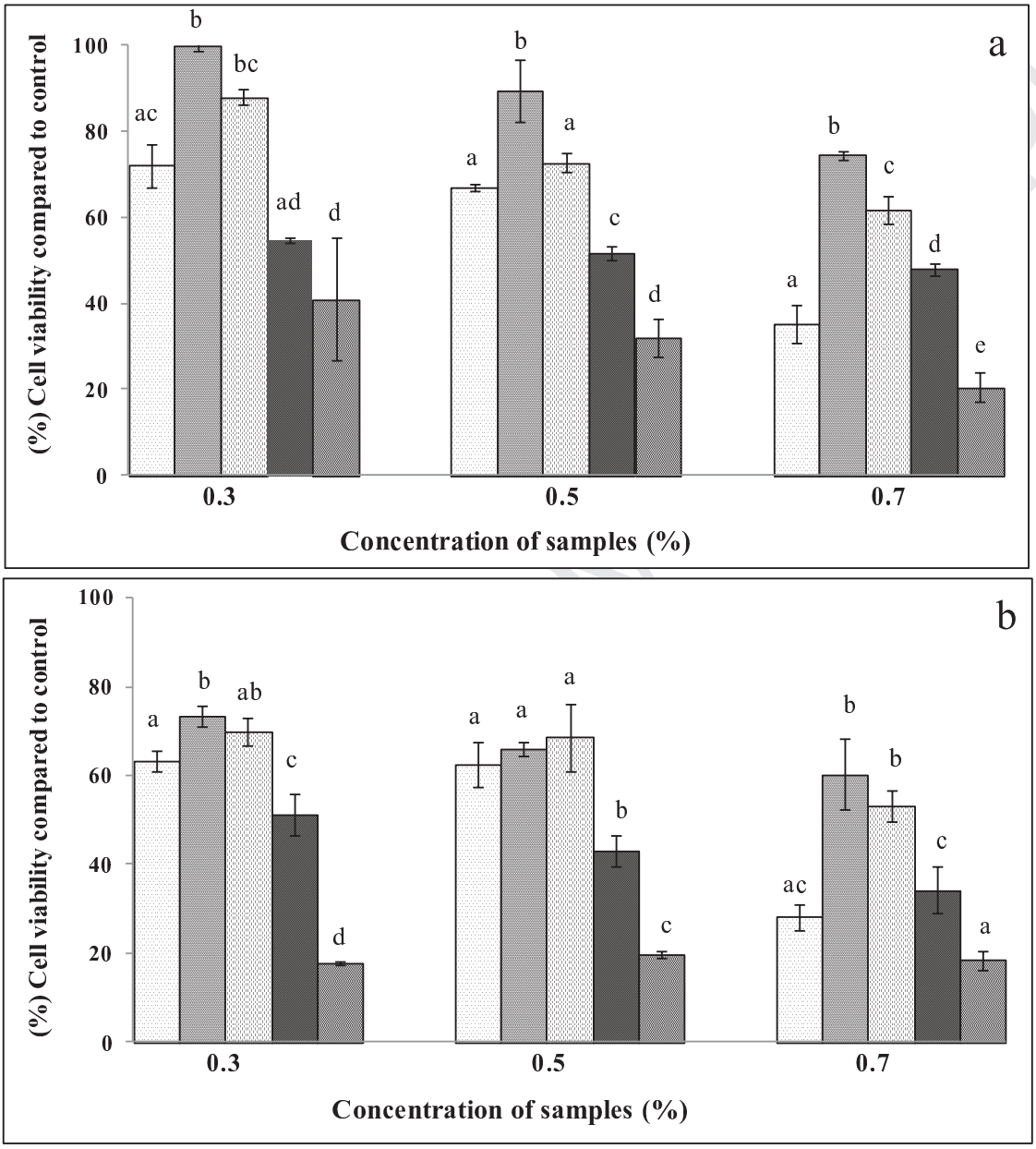

Table 1. Percentage growth inhibition of MDR *E.cloacae* WT6 and MRSA ATCC43300 bacteria on the test sol-gel coatings with doping levels of 0.5% and 0.3 % (w/w).

	Percentage (%) growth inhibition			
	Enterobacter cloacae WT6		MRSA ATCC 43300	
Samples	0.3%	0.5%	0.3%	0.5%
Cca	2.94 ± 1.3^{a}	4.3 ± 3.1^{a}	1.2 ± 00^{a}	12.26 ± 1.3^{a}
AgC	9.2 ± 2.7^{ab}	95.5 ± 8.7^{b}	10.40 ± 1.3^{b}	93.5 ± 7.8^{b}
Ag6	17.9 ± 1.3^{bc}	100 ± 0.0^{b}	19.80 ± 4.0^{c}	94.2 ± 9.7^{b}
Ag7	25.6 ± 0.1^{c}	97.5 ± 6.1^{b}	31.60 ± 4.9^{d}	98.4 ± 3.8^{b}
Ag8	42.1 ± 4.3^{d}	100 ± 0.0^{b}	46.20 ± 1.3^{e}	96.7 ± 4.4^{b}
AgN	47.9 ± 7.1^{d}	89.3 ± 2.3^{c}	66.0 ± 1.2^{f}	99.5 ± 5.9^{b}

The letters (a-f) at each concentration indicate groups that are significantly different ($P < 0.05$)

Table 2. Value of model parameters [Lag phase (λ) and maximum specific growth rate (μ_{max})] for the non-linear regression of Gompertz equation for fitting of bacterial growth

*E.cloacae*WT6	λ (h)	$\mu_{max}(h^{-1})$	R^2
Control	5.89 ± 0.04	0.32 ± 0.00	0.996
AgC	6.96 ± 0.04	0.19 ± 0.01	0.998
Ag6	8.66 ± 1.22	0.17 ± 0.03	0.994
Ag7	9.14 ± 0.31	0.15 ± 0.01	0.996
Ag8	9.70 ± 0.45	0.14 ± 0.02	0.997
AgN	10.26 ± 0.49	0.12 ± 0.02	0.991
MRSA ATCC 43300			
Control	2.79 ± 1.22	0.22 ± 0.02	0.990
AgC	4.88 ± 0.76	0.18 ± 0.05	0.990
Ag6	6.28 ± 0.10	0.14 ± 0.01	0.993
Ag7	7.41 ± 1.44	0.13 ± 0.01	0.986
Ag8	8.14 ± 0.08	0.13 ± 0.0	0.984
AgN	7.79 ± 1.29	0.01 ± 0.01	0.994

Table 3. Summary of XPS data, before and after exposure to *S. epidermidis* broth for four days

	Atomic %							
Coating type		**C**		**O**	**Si**	**Ag**	**N**	**Na**
	C–C	C–N/ C–O	N–C=O/ O–C=O					
AgN		**28.3**		**43.1**	**27.8**	**0.8**	**0.0**	**0.0**
	(27.4)	(0.9)	(0)					
Ag8		**28.5**		**45.1**	**26.3**	**0.1**	**0.0**	**0.0**
	(27.9)	(0.6)	(0)					
AgN-after exposure		**46.0**		**31.4**	**14.0**	**0.2**	**6.7**	**1.6**
	(28.1)	(11.3)	(6.6)					
Ag8-after exposure		**46.3**		**32.0**	**16.2**	**0.1**	**5.0**	**0.4**
	(31.9)	(9.2)	(5.2)					